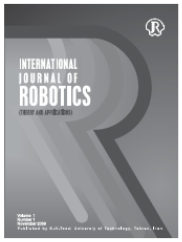

INTERNATIONAL JOURNAL OF ROBOTICS
(THEORY AND APPLICATIONS)
E-mail: IJR@kntu.ac.ir

Hybrid Concepts of the Control and Anti-Control of Flexible Joint Manipulator

Maysam Zamani Pedram[a]*, Mahdi Aliyari Shoorehdeli[a], Faezeh Farivar[b], Mojtaba Rostami Kandroodid[c]

a-Faculty of Electrical Engineering, Department of Mechatronics Engineering, K. N. Toosi University of Technology, Tehran, Iran. Maysam_pedram@ee.kntu.ac.ir, Aliyari@eetd.kntu.ac.ir
b-Faculty of Engineering, Department of Mechatronics Engineering, Science and Research Branch, Islamic Azad University, Tehran, Iran, F.Farivar@srbiau.ac.ir.
c-Faculty of Electrical and Computer Engineering, Department of Control Engineering, University of Tehran, Tehran, Iran, M.rostami.k@ece.ut.ac.ir.

ARTICLE INFO

Keywords:
Gaussian RBF neural network
Sliding mode control
Switching surface
Anti- control
Chaos
Synchronization
Flexible Joint
Chaotic Gyroscope

ABSTRACT

This paper presents a Gaussian radial basis function neural network based on sliding mode control for trajectory tracking and vibration control of a flexible joint manipulator. To study the effectiveness of the controllers, designed controller is developed for tip angular position control of a flexible joint manipulator. The adaptation laws of designed controller are obtained based on sliding mode control methodology without calculating the Jacobian of the flexible joint system. Also in this study, the anti-control is applied to reduce the deflection angle of flexible joint system. To achieve this goal, the chaos dynamic must be created in the flexible joint system. So, the flexible joint system has been synchronized to chaotic gyroscope system. In this study, control and anti-control concepts are applied to achieve the high quality performance of flexible joint system. It is tried to design a controller which is capable to satisfy the control and anti- control aims. The performances of the proposed control are examined in terms of input tracking capability, level of vibration reduction and time response specifications. Finally, the efficacy of the proposed method is validated through experimentation on QUANSER's flexible-joint manipulator.

1. Introduction

The trajectory tracking control of robotic manipulators with joint flexibility has received considerable attention, owing to the complexity of the problem. Many robots incorporate harmonic drives for speed reduction, and it is known that such drives introduce torsional elasticity into the joints [1]. Industrial robots generally have elastic elements in the transmission systems, which may result in the occurrence of torsional vibrations when a fast response is required. For many manipulators, joint elasticity may arise from several sources, such as elasticity in gears, belts, tendons, bearings, hydraulic lines, etc., and may limit the speed and dynamic accuracy achievable by control algorithms designed assuming perfect rigidity at joints. A proper choice of mathematical model for a control system design is a crucial stage in the development of control strategies for any system. This is particularly true for robotic manipulators due to their complicated dynamics [2].

Experimental evidence suggests that joint flexibility should be taken into account in both modeling and control of manipulators if high performance is to be achieved. To model this elastic behavior in the joints, the link is considered as connected to rotor through a torsional spring of stiffness K. The introduction of joint flexibility in the robot model considerably complicates the equations of motion. In particular, the order of the related dynamics becomes twice that of the rigid robots, and the number of degrees of freedom is larger than the number of inputs, making the control task difficult. Research on the dynamic modeling and control of flexible robots has received increased attention in the last decades. A first

step towards designing an efficient control strategy for manipulators with flexible joints must be aimed at developing dynamic models that can characterize the flexibility of the joints accurately. The controller design that minimizes the effects of the flexible displacements in lightweight robots is highly demanded in many industrial and space applications that require accurate trajectory control. In control applications of robot manipulators with flexible arms are targeted either to reach a target position or to follow a prescribed trajectory. In the first case to reach a target position, a short settling time is desired while a large robot arm displacement is planned in the second case to follow a prescribed trajectory. In both case, strong control actions are applied to the robot arm and as a result, undesired behaviors could appear if vibrations induced in the robot arm are not considered [3].

The control issue of the flexible joint is to design the controller so that link of robot can reach a desired position or track a prescribed trajectory precisely with minimum vibration to the link. In order to achieve these objectives, various methods using different technique have been proposed such as follow:

Linear quadratic regulation (LQR) control [4], Adaptive output-feedback controller based on a backstepping design [5-7], Nonlinear control based on feedback linearization technique and the integral manifold technique [8,9], Robust control based on PD control [10], and robust H_∞ control [11], Fuzzy control, PD fuzzy and Neural network [12-15] , Optimal control [16, 17], etc [2, 18-22].

In this paper, Gaussian radial basis function neural network (RBFNN) based on sliding mode control is designed to control of flexible joint system. The adaptation laws of RBFNN are obtained based on sliding mode control methodology without calculating the Jacobian of the system. Also, anti-control is applied in this study to reduce the deflection angle of flexible joint system. It means that the chaotic dynamic can be useful to control of flexible joint system as an anti- control (More details are presented in section IV). In this study, to create the chaos dynamic in the flexible joint system, this system can be synchronized to the chaotic gyroscope system. Therefore, control and anti-control are applied to achieve the high quality performance of flexible joint system. It is tried to design a controller which is capable to satisfy the control and anti- control aims. The designed controller has been implemented on the QUANSER flexible joint system.

The advantages of this proposed method to control of flexible joint not considered in previous study are mentioned as follow:

This method is capable to reduce the deflection angle of the flexible link with considering the scale of reduction. The global stability of the system is guaranteed while the system is synchronized with a chaotic system. The proposed control method is robust due to be sliding surface and sliding mode control in proposed control method.

This paper is organized as follows: The flexible joint manipulator and modelling of this system are described in section II. Control problem formulation is presented in Section III. In section IV, chaos in flexible joint and chaos synchronization are explained. Also, chaotic gyroscope system is described in this section. In section V, the RBFNN based on sliding mode control is designed. The switching surfaces and learning algorithm of RBFNN are presented in this section. Finally, the implementation and results obtained from QUANSER flexible joint system are presented to show the effectiveness of proposed control method in section VI. At the end, the paper is concluded in section VII.

2. Description of The Flexible Joint Manipulator

The flexible joint manipulator system considered in this work is shown in Fig. 1, where θ is the tip angular position and α is the deflection angle of the flexible link. The base of the flexible joint manipulator which determines the tip angular position of the flexible link is driven by servomotor, while the flexible link will response based on base movement. The deflection of link will be determined by the flexibility of the spring as their intrinsic physical characteristics [23].

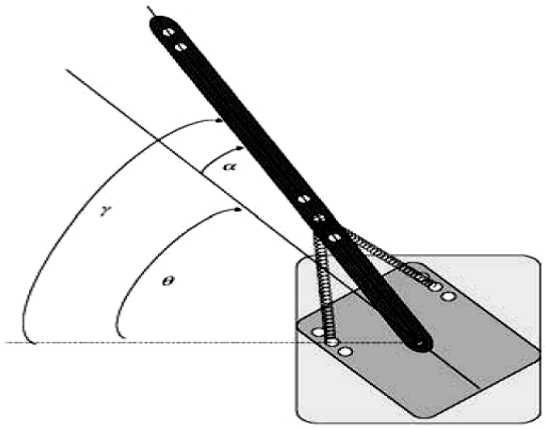

Fig.1. Flexible Joint Manipulator System.

A. Modeling of the System

This section provides a brief description on the modeling of the flexible joint manipulator system, as a basis of a simulation environment for development and assessment of the nonlinear control. The Euler-Lagrange formulation is considered in characterizing the dynamic behavior of the system. Considering the motion of the flexible joint system on a two-dimensional plane, the potential energy of the spring can be formulated as [23]:

$$V = \frac{1}{2} K_{stiff} \alpha^2 \quad (1)$$

where K_{stiff} is the joint stiffness. The kinetic energies in the system arise from the moving hub and flexible link can be formulated as:

$$T = \frac{1}{2} J_{eq} \dot{\theta}^2 + \frac{1}{2} J_{Arm} \left(\dot{\theta} + \dot{\alpha} \right)^2 \tag{2}$$

where J_{eq} and J_{Arm} are the equivalent inertia and total link inertia, respectively. To obtain a closed-form dynamic model of the flexible joint, the energy expressions in Eq. (1) and Eq. (2) are applied to formulate the Lagrangian, that is:

$$L = T - V = \frac{1}{2} J_{eq} \dot{\theta}^2 + \frac{1}{2} J_{Arm} \left(\dot{\theta} + \dot{\alpha} \right)^2 - \frac{1}{2} K_{stiff} \alpha^2 \tag{3}$$

Two generalized co-ordinates are θ and α. Let the generalized torque corresponding to the generalized tip angle be $T_{output} - B_{eq} \dot{\theta}$. Using Lagrangian's equation as follow:

$$\frac{\partial}{\partial t} \left(\frac{\partial L}{\partial \dot{\theta}} \right) - \frac{\partial L}{\partial \theta} = T_{output} - B_{eq} \dot{\theta} \tag{4}$$

$$\frac{\partial}{\partial t} \left(\frac{\partial L}{\partial \dot{\alpha}} \right) - \frac{\partial L}{\partial \alpha} = 0 \tag{5}$$

The equation of motion is obtained as below:

$$J_{eq} \ddot{\theta} + J_{Arm} \left(\ddot{\theta} + \ddot{\alpha} \right) = T_{output} - B_{eq} \dot{\theta} \tag{6}$$

$$J_{Arm} \left(\ddot{\theta} + \ddot{\alpha} \right) + K_{stiff} \alpha = 0 \tag{7}$$

where B_{eq} is the equivalent viscous damping and T_{output} is the output torque on the load from the motor, defined as:

$$T_{output} = \frac{\eta_m \eta_g K_t K_g \left(V_m - K_g K_m \dot{\theta} \right)}{R_m} \tag{8}$$

where η_m is the motor efficiency, η_g is the gearbox efficiency, K_t is the motor torque constant, K_g is the high gear ratio, K_m is the motor back-EMF constant and R_m is the armature resistance. The linear model of the uncontrolled system can be represented in a state-space form as shown in equation Eq. (9), that is:

$$\begin{cases} \dot{x}_1 = x_3 \\ \dot{x}_2 = x_4 \\ \dot{x}_3 = a x_2 + b x_3 + c u \\ \dot{x}_4 = d x_2 + f x_3 - c u \end{cases} \tag{9}$$

where $x = [\theta \quad \alpha \quad \dot{\theta} \quad \dot{\alpha}]^T$, and a , b , c , d and f are given as:

$$\begin{cases} a = \dfrac{K_{stiff}}{J_{eq}} \\ b = \dfrac{-\eta_m \eta_g K_t K_m K_g^2 + B_{eq} R_m}{J_{eq} R_m} \\ c = \dfrac{\eta_m \eta_g K_t K_g}{J_{eq} R_m} \\ d = -\dfrac{K_{stiff} \left(J_{eq} + J_{Arm} \right)}{J_{eq} J_{Arm}} \\ f = \dfrac{\eta_m \eta_g K_t K_m K_g^2 + B_{eq} R_m}{J_{eq} R_m} \end{cases} \tag{10}$$

In Eq. (9), the input u is the input voltage of the servomotor, V_m which determines the flexible joint manipulator base movement. In this study, the values of the parameters are defined as Table.1. Directions of torque to reduce the deflection angle when link moves anti-clockwise and clockwise are shown in Fig.2 (a) and Fig. 2 (b), respectively.

3. Control Problem Formulation

In the previous section, it has been shown that the flexible joint system can be considered as an under-actuated system. In order to improve the performance of the dynamic system, we need to control the flexible joint system with a suitable motion which is beneficial for working with a particular condition. It is thus of great practical importance to develop suitable control methods. For this purpose, in this section, control problem of the flexible joint system is formulated. The control aims are that:

TABLE.1: SYSTEM PARAMETERS

Symbol	*Quantity*	*value*
R_m	Armature Resistance (Ω)	2.6
K_m	Motor Back-EMF Constant $(V.rad/S)$	0.00767
K_t	Motor Torque Constant $(N.M/A)$	0.00767
J_{Arm}	Total Arm Inertia $\left(kg.m^2\right)$	0.0035
J_{eq}	Equivalent Inertia $\left(kg.m^2\right)$	0.0026
K_g	High Gear Ratio	14:5
K_{stiff}	Joint Stiffness	1.2485
B_{eq}	Equivalent Viscous Damping $(N.M.S/rad)$	0.004
η_g	Gearbox Efficiency	0.9
η_m	Motor Efficiency	0.69

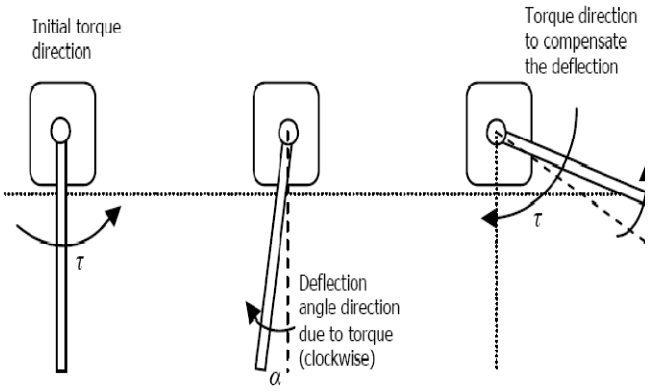

Fig.2 (a): Direction of torque to reduce deflection angle when link moves anti-clockwise.

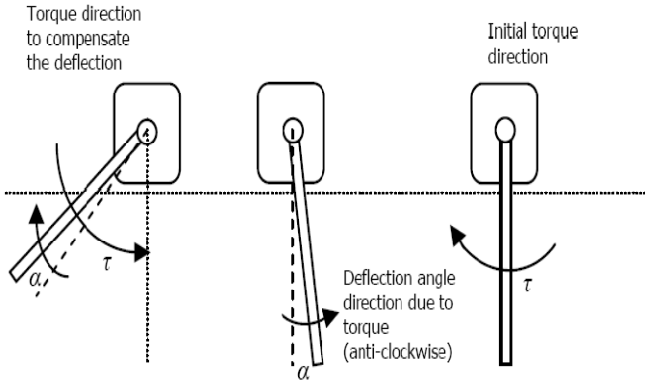

Fig.2 (b): Direction of torque to reduce deflection angle when link moves clockwise.

(1)Tracking the desired tip angular position, (2) Minimizing the deflection angle.

Therefore, the control problem is to drive the system to track a four-dimensional desired vector $X_d(t)$ as follows:

$$X_d(t)=[x_{d-1},x_{d-2},x_{d-3},x_{d-4}]^T=[x_{d-1},x_{d-2},\dot{x}_{d-1},\dot{x}_{d-2}]^T \quad (11)$$

, which belongs to a class of C function on $[t_0,\infty)$. Let us define the tracking error as:

$$\begin{cases} e_c = x_1 - x_{d\_1} \\ e_s = x_2 - x_{d\_2} \end{cases} \quad (12)$$

Then, the error dynamics can be obtained from Eq. (12) and Eq. (9) as follow:

$$\begin{cases} \dot{e}_c = \dot{x}_1 - \dot{x}_{d\_1} = x_3 - \dot{x}_{d\_1} \\ \dot{e}_s = \dot{x}_2 - \dot{x}_{d\_2} = x_4 - \dot{x}_{d\_2} \end{cases} \quad (13)$$

To achieve the control input, it is necessary to differentiate Eq. (13). From Eq. (13) and Eq. (9), we obtain:

$$\begin{cases} \ddot{e}_c = \dot{x}_3 - \ddot{x}_{d\_1} = \underbrace{ax_2 + bx_3 - \ddot{x}_{d\_1}}_{g_1(x_2,x_3,x_{d-1})} + cu \\ \quad = g_1(x_2,x_3,x_{d-1}) + cu \\ \ddot{e}_s = \dot{x}_4 - \dot{x}_{d\_2} = \underbrace{dx_2 + fx_3 - \dot{x}_{d\_2}}_{g_2(x_2,x_3,x_{d-2})} - cu \\ \quad = g_2(x_2,x_3,x_{d-2}) - cu \end{cases} \quad (14)$$

Therefore, the control problem can be formulated as follow:

$$\begin{cases} \dot{e}_{c1} = e_{c2} \\ \dot{e}_{c2} = g_1(x_2,x_3,x_{d-1}) + cu \\ \dot{e}_{s1} = e_{s2} \\ \dot{e}_{s2} = g_2(x_2,x_3,x_{d-2}) - cu \end{cases} \quad (15)$$

Define the error vector as:

$$E(t)=[e_{c1}(t),e_{c2}(t),e_{s1}(t),e_{s2}(t)]^T \quad (16)$$

The control goal considered in this section is that for any given target orbit $X_d(t)$, the controller is designed such that the resulting tracking error vector satisfies:

$$\lim_{t\to\infty}\|E(t)\|\to 0 \quad (17)$$

where $\|\cdot\|$ is the Euclidean norm of a vector.

4. Chaos in Flexible Joint

In the previous section, the control aims have been explained. In this study, the desired vector $X_d(t)$ will be considered as follow: (1) x_{d-1} is the trajectory of the reference input such as pulse and sinusoid trajectories shown in result section. (2) x_{d-2} is considered as a proportional trajectory of a chaotic mechanical system such as a chaotic gyroscope system. This choice has been proposed to use the properties of chaotic systems described in the next section.

a. Chaos Synchronization to Control of Flexibel Joint

Dynamic chaos is a very interesting nonlinear effect which has been intensively studied during the last three decades. Chaos control can be mainly divided into two categories [24]: one is the suppression of the chaotic dynamical behavior and the other is to generate or enhance chaos in nonlinear system.

In this study, chaos synchronization [25] has been suggested to create the chaotic behavior in the flexible joint system. Basically, the chaos synchronization problem means making two systems oscillate in a synchronized manner. Given a chaotic system considered as the master system, and another system considered as the slave system, the dynamical behaviors of these two systems may be identical after a transient time when the slave system is driven by a control input. Different types

of synchronization have been found in interacting chaotic systems, such as generalized projective synchronization that the master and slave vectors synchronize up to a constant scaling factor α (a proportional relation) [26-28].

In this study, the flexible joint system and the chaotic gyroscope system have been considered as the slave and the master systems, respectively.

Notice that, the second state of the flexible joint will be synchronized to the second state of the chaotic gyroscope system. This synchronization is the generalized projective synchronization with a constant scaling factor α . So,

$$x_{d-2} = \alpha x_{2gyro} \tag{18}$$

where α is very small scalar value in the range of 10^{-n}, $3 < n < 5$.

In this section, chaos synchronization is used as the anti-control to control of the flexible joint system. In the next part, dynamics of the chaotic gyroscope system are described.

b. Chaotic Gyroscope System

The symmetric gyroscope mounted on a vibrating base is shown in Fig. 3. The dynamics of a symmetrical gyro with linear-plus-cubic damping of angle θ can be expressed as [29]:

$$\ddot{\theta}+\alpha^2\frac{(1-\cos\theta)^2}{\sin^3\theta}-\beta\sin\theta+c_1\dot{\theta}+c_2\dot{\theta}^3 = f\sin\omega t\sin\theta \tag{19}$$

where $f\sin\omega t$ is a parametric excitation, $c_1\dot{\theta}$ and $c_2\dot{\theta}^3$ are linear and nonlinear damping terms, respectively and $\alpha^2((1-\cos\theta)^2/\sin^3\theta)-\beta\sin\theta$ is a nonlinear resilience force. According to [29], in a symmetric gyro mounted on a vibrating base, the precession and the spin angles have cyclic motions and hence their momentum integrals are constant and equal to each other. So the governing equations of motion depend only on the mutational angle θ. Using Routh's procedure and assuming a linear-plus-cubic form for dissipative force, Eq. (19) is obtained [29]. Given the states $x_1 = \theta$ and $x_2 = \dot{\theta}$ and $g(\theta) = \alpha^2((1-\cos\theta)^2/\sin^3\theta)-\beta\sin\theta$, Eq. (19) can be rewritten as:

$$\begin{cases}\dot{x}_1 = x_2\\ \dot{x}_2 = g(x_1)-c_1x_1-c_2{x_2}^3+(\beta+f\sin\omega t)\sin(x_1)\end{cases} \tag{20}$$

This gyro system exhibits complex dynamics and has been studied by [29] for values of f in the range $32 < f < 36$ and constant values of $\alpha^2 = 100$, $\beta = 1$, $c_1 = 0.5$, $c_2 = 0.05$ and $\omega = 2$. Fig. 4 illustrate the irregular motion exhibited by this system for $f = 35.5$ and initial conditions of $(x_1, x_2) = (1,-1)$.

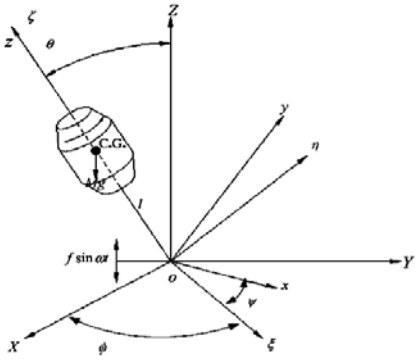

Fig. 3: A schematic diagram of a symmetric gyroscope.

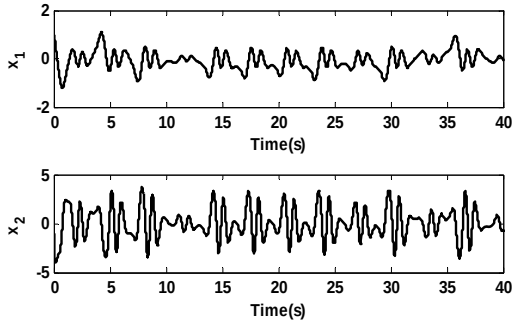

Fig.4: Time series of x_1 and x_2 .

In the next section, the control input will be obtained via Gaussian RBF neural network to achieve the control objective presented in previous section. Also, the learning algorithm of RBFNN based on sliding mode control is presented in the next section.

5. Gaussian RBF Neural Network Control Based on Sliding Mode Control

Gaussian radial basis function neural network (GRBFNN) can be applied to control of flexible joint. The architecture of GRBFNN based on sliding mode control of the flexible joint system is shown in Fig.5. The inputs of GRBFNN are sliding surfaces presented in the part *B* in this section.

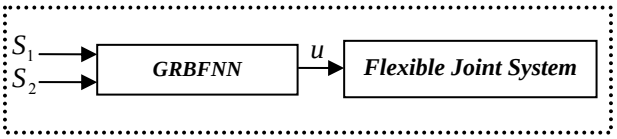

Fig.5: GRBFNN based on sliding mode control of the flexible joint system.

B. GRBF Neural Network

The network structure of the $GRBF_{NN}$ is shown in Fig. 6, which can be considered as one layer feed forward neural network with nonlinear element. The $GRBF_{NN}$ output can perform the mapping according to:

$$f(z)=\sum_{j=1}^{n} w_j G_j(z_j,m_j,\sigma_j) \tag{21}$$

where $z=[z_1,z_2,...,z_n]^T \in R^n$ is the input vector, $G_j(z_j,m_j,\sigma_j)\in R^n, j=1,2,...,n$ are the Gaussian radial basis function, $\sigma_j \in R$ is the spread of Gaussian function, m_j is the mean value of Gaussian function and n is the number of neurons. Each Gaussian radial basis function can be represented by:

$$G_j(z_j,m_j,\sigma_j)=\exp\left(\frac{z_j-m_j}{\sqrt{2}\sigma_j}\right)^2 \tag{22}$$

Notice that the optimal values are not unique.

In this study, m and σ are not trained. The input vector z is $[S_1,S_2]$ and the $GRBF_{NN}$ output f is considered as the control input u.

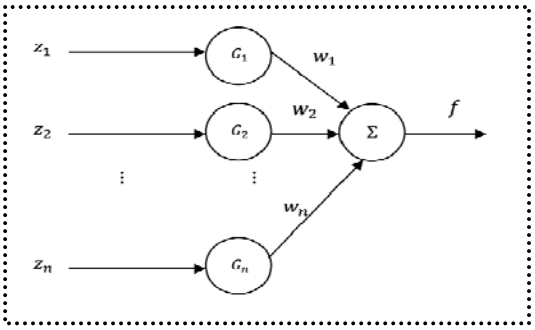

Fig.6: Structure of GRBF neural network

C. Switching Surface

Using the sliding mode control method to control the flexible joint system, involves two basic steps; (1) Selecting an appropriate sliding surface such that the sliding motion on the sliding manifold is stable and ensures $\lim_{t\to\infty}\|E(t)\|\to 0$. (2) Establishing a robust control law which guarantees the existence of the sliding manifold $S(t)=0$. The sliding surfaces are defined as [30]:

$$S(t)=\left(\frac{d}{dt}+\delta\right)^{n-1} e(t) \tag{23}$$

where $S(t)\in R$ and δ is a real positive constant parameter. Differentiating Eq. (23) with respect to time as follow:

$$\dot{S}(t)=\left(\frac{d}{dt}+\delta\right)^{n} e(t) \tag{24}$$

The rate of convergence of the sliding surface is governed by the value assigned to parameter δ. Having established appropriate sliding surfaces, the next step is to design the control input to drive the error system trajectories onto the sliding surfaces.

In this study, define two sliding surfaces as:

$$S_1(t)=e_{c2}(t)+\delta_1 e_{c1}(t) \tag{25}$$

$$S_2(t)=e_{s2}(t)+\delta_2 e_{s1}(t) \tag{26}$$

Eq. (25) and Eq. (26) are designed as the input of GRBFNN. Differentiating Eq. (25) and Eq. (26) with respect to time as follow:

$$\dot{S}_1(t)=\dot{e}_{c2}(t)+\delta_1 \dot{e}_{c1}(t) \tag{27}$$

$$\dot{S}_2(t)=\dot{e}_{s2}(t)+\delta_2 \dot{e}_{s1}(t) \tag{28}$$

Substituting Eq. (15) into Eq. (27) and Eq. (28), then we obtain:

$$\dot{S}_1(t)=g_1(\cdot)+\delta_1 e_{c2}+cu \tag{29}$$

$$\dot{S}_2(t)=g_2(\cdot)+\delta_2 e_{s2}-cu \tag{30}$$

D. Learning Algorithm

Define the cost function as follow:

$$E=S_1\dot{S}_1+S_2\dot{S}_2 \tag{31}$$

where S_1 and S_2 are presented in Eq. (23) and Eq. (24).

By using Back-Propagation (BP) algorithm, the weighting vector of the RBFNN is adjusted such that the cost function defined in Eq. (31) is less than a designed. The well-known algorithm may be written briefly as:

$$w(k+1)=w(k)-\eta\frac{\partial E}{\partial w} \tag{32}$$

where η and w represent the learning rate and tuning parameter of RBFNN. The gradient of E in Eq. (32) with respect to the weighting vector w can be obtained as follow:

$$\frac{\partial E}{\partial w}=\frac{\partial\left(S_1\dot{S}_1\right)}{\partial w}+\frac{\partial\left(S_2\dot{S}_2\right)}{\partial w}=S_1\frac{\partial\dot{S}_1}{\partial w}+S_2\frac{\partial\dot{S}_2}{\partial w} \tag{33}$$

Eq. (33) can be rewritten as follow:

$$\frac{\partial E}{\partial w}=S_1\frac{\partial\dot{S}_1}{\partial u}\frac{\partial u}{\partial w}+S_2\frac{\partial\dot{S}_2}{\partial u}\frac{\partial u}{\partial w} \tag{34}$$

With considering Eq. (29) and Eq. (30), Eq.(28) can be simplified as follow:

$$\frac{\partial E}{\partial w} = c\left(S_1 - S_2\right)G \tag{35}$$

where c and G are presented in Eq. (10) and Eq. (22).

Therefore, the adaptation law of GRBFNN is obtained as:

$$w(k+1) = w(k) - \eta c\left(S_1 - S_2\right)G \tag{36}$$

6. IMPLEMENTATION AND RESULTS

In this section, the proposed control has been implemented and tested within the simulation environment of the flexible joint manipulator and the corresponding results are presented.

The control signal generated has been applied to the flexible joint manipulator through QUANSER's interfacing hardware board. The fourth order Runge–Kutta algorithm are applied to solve the sets of differential equations related to the systems with a time grid of 0.001.

The system responses namely the tip angular position and deflection angle are observed. The performances of the designed control are assessed in terms of vibration suppression, trajectory tracking and input control. Moreover, time response specifications are summarized on Table.2. Finally, a comparative assessment of the performance of the control schemes is presented and discussed.

The parameters of designed control are:

$\delta_1 = 2.9$, $\delta_2 = 28$, $\eta = .00001$, $\alpha = 0.0001$ $n = 5 neurons$, $m = [-3 \quad -1.5 \quad 0 \quad 1.5 \quad 3]$, and $\sigma = 35$.

Implementation results have been investigated as follow:

a) *The flexible joint manipulator is required to follow a pulse-trajectory of 28.65º* (=0.5 rad) *and 57.30º* (=1 rad) *with the frequency 0.1Hz.*

Fig.7 and Fig.8 are corresponding to a pulse-trajectory of 28.65º and 57.30º, respectively. As Fig. 7(a) shows the flexible joint manipulator tracks the pulse-trajectory of 30º. Fig 7(b) demonstrates deflection angle. It is observable that deflection angle amplitude's range is satisfactory and it has a suitable damping ratio. The control input is shown in Fig. 7(c). As Fig. 8(a) shows the flexible joint manipulator tracks the pulse-trajectory of 60º. Fig 8(b) demonstrates deflection angle. It is observable that deflection angle amplitude's range is satisfactory and it has a suitable damping ratio. The control input is shown in Fig. 8 (c).

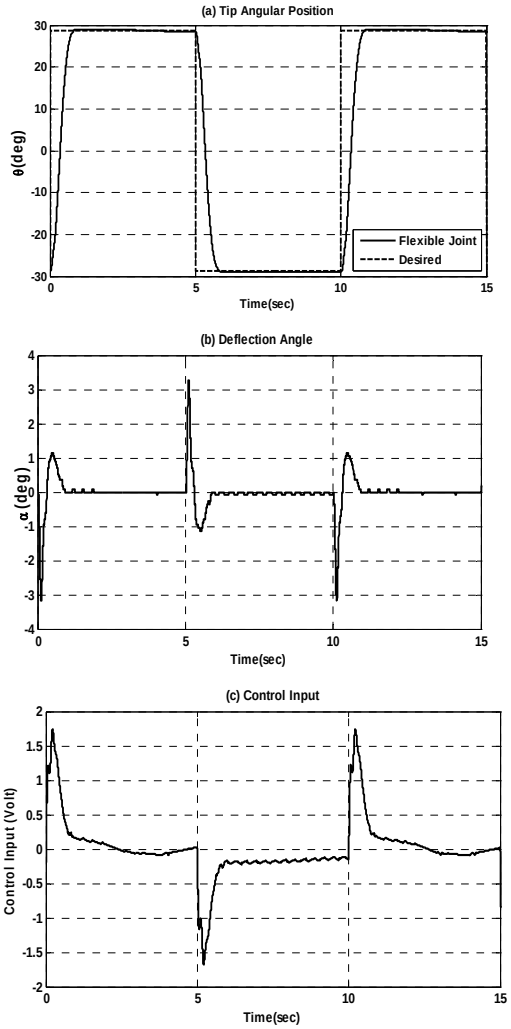

Fig.7: (Desrired: pulse-trajectory of 28.65º) (a) Tip angular position of the flexible joint manipulator, (b) Deflection angle the flexible joint manipulator, (c) Control input.

Fig.9 and Fig.10 are corresponding to a sinusoid-trajectory of 28.65º and 57.30º with the frequency 0.1Hz, respectively. As Fig. 9(a) shows the flexible joint manipulator tracks the sinusoid-trajectory of 30º. Fig 9(b) demonstrates deflection angle. It is observable that deflection angle amplitude's range is satisfactory and it has a suitable damping ratio. The control input is shown in Fig. 9(c). As Fig. 10(a) shows the flexible joint manipulator tracks the sinusoid-trajectory of 60º. Fig 10(b) demonstrates deflection angle. It is observable that deflection angle amplitude's range is satisfactory and it has a suitable damping ratio. The control input is shown in Fig. 10(c).

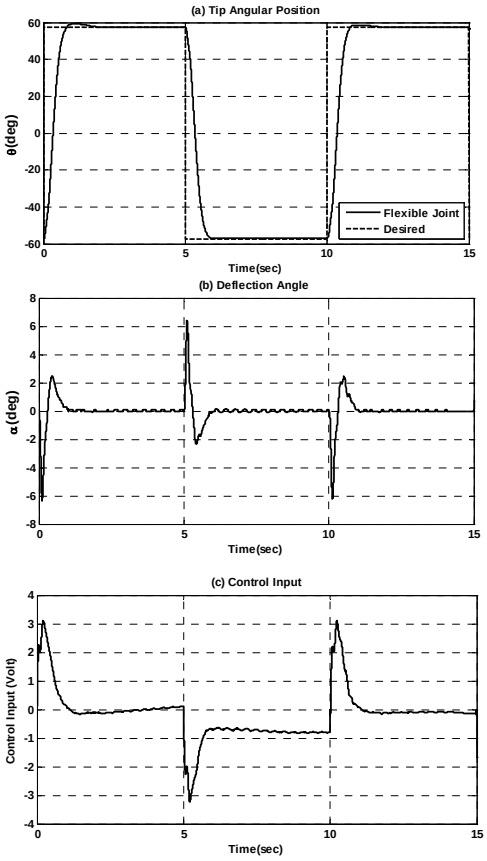

Fig.8: (Desired: pulse-trajectory of 57.30º)
(a) Tip angular position of the flexible joint manipulator, (b) Deflection angle the flexible joint manipulator, (c) Control input.

b) **The flexible joint manipulator is required to follow a sinusoid-trajectory with amplitude 28.65º (=0.5 rad) and 57.30º (=1 rad) with the frequency 0.1Hz.**

It is noted that the flexible joint manipulator reaches the required position within 0.5 sec, with little overshoot. However, a noticeable amount of vibration occurs during movement of the manipulator. It is noted from the deflection angle response that the vibration of the system settles within 1 sec with a maximum deflection angle of ±6°.

The obtained results have been demonstrated that designed controller provide higher level of vibration reduction as compared to some studies such as [13, 16, 17]. Also, the high performance of input tracking has been achieved. The speed of the response is slightly improved at the expenses of decrease in the level of vibration reduction. It is concluded that the proposed controller is capable of reducing the system vibration while maintaining the input tracking performance of the manipulator. Therefore, the proposed control is capable of reducing the system vibration while maintaining the trajectory tracking performance of the manipulator.

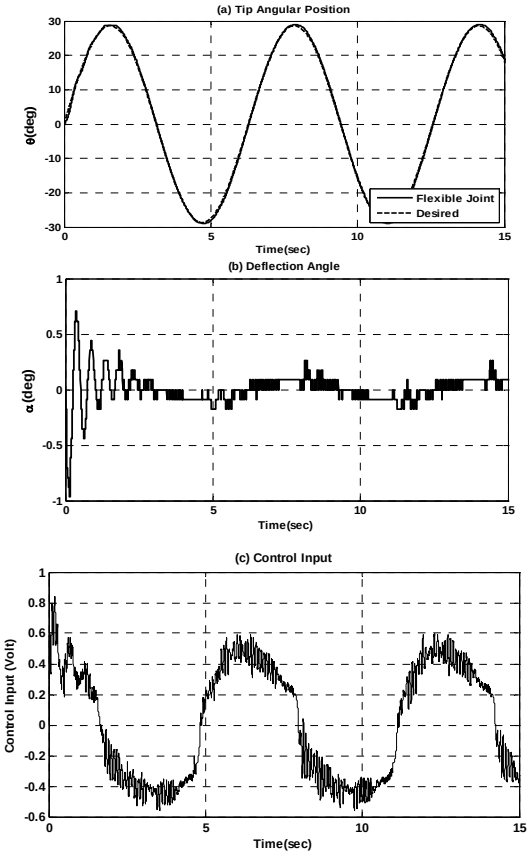

Fig.9: (Desired: sinusoid-trajectory with amplitude of 28.65º)
(a) Tip angular position of the flexible joint manipulator, (b) Deflection angle the flexible joint manipulator, (c) Control input.

7. Conclusions

In this paper, a Gaussian RBFNN based on sliding mode control has been designed for trajectory tracking control of flexible joint manipulator system. The development of designed control and vibration suppression of a flexible joint manipulator have been presented. The anti-control concept is applied to reduce the deflection angle of flexible joint system. So, the chaos dynamic must be created in the flexible joint system and the flexible joint system has been synchronized to chaotic gyroscope system. Therefore, the control and anti-control concepts are applied to achieve the high quality performance of flexible joint system.

The performances of the control schemes have been evaluated in terms of input tracking capability, level of vibration reduction, time response specifications.

Experimental results have shown that the proposed approach is effective in practice. Acceptable performance in input tracking control and vibration suppression has been achieved with designed controllers. Moreover, a significant reduction in the system vibration has been achieved with the anti-control concepts. The obtained results have been demonstrated that designed controller provide higher level of vibration reduction as compared to some studies such as [13, 16, 17]. Also, the high

performance of input tracking has been achieved. The speed of the response is slightly improved at the expenses of decrease in the level of vibration reduction. It is concluded that the proposed controller is capable of reducing the system vibration while maintaining the input tracking performance of the manipulator.

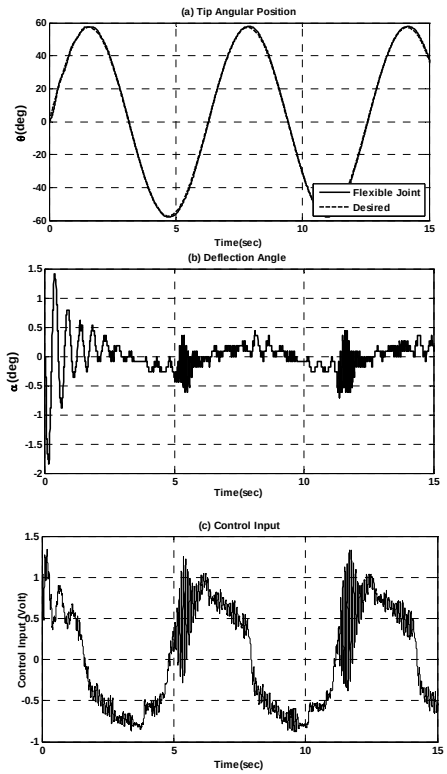

Fig.10: (Desired: sinusoid-trajectory with amplitude of 57.30º) (a) Tip angular position of the flexible joint manipulator, (b) Deflection angle the flexible joint manipulator, (c) Control input.

TABLE.2: MAGNIYUDE OF SPECIFICATIONS OF TIP ANGULAR POSITION

		Desired Trajectories			
Magnitude (deg)		Pulse 28.65º	Pulse 57.30º	Sinusoid 28.65º	Sinusoid 57.30º
Specifications of tip angular position response	Settling time (Sec)	1	1.03	Not Defined	Not Defined
	Rise time (Sec)	0.23	0.47	Not Defined	Not Defined
	Overshoot (Percent %)	0	2	Not Defined	Not Defined

ACKNOWLEDGMENT

Authors are much grateful to Dr M.Teshnehlab, the director of the intelligent system laboratory (ISLAB) of K. N. Toosi University for his support of this study.

REFERENCES

[1] M. W. Spong and M. Vidyasagar, "Robot Dynamics and Control", New York: Wiley, 1989.

[2] S. E. Talole, J. P. Kolhe, S. B. Phadke, "Extended-State-Observer-Based Control of Flexible-Joint System With Experimental Validation", *IEEE Trans on Industerial Electronics*, Vol. 57, No. 4, pp. 1411-1419, 2010.

[3] F. M. Botsali, M. kalyancu, M. Tinkir, U. Onen, " Fuzzy Logic Trajectory Control of Flexible Robot Manipulator With Rotating Prismatic Joint", *2nd international Conference on computer and automation engineering (ICCAE)*, pp.35-39, 2010.

[4] M. A. Ahmad, "Vibration and Input Tracking Control of Flexible Manipulator using LQR with Non-collocated PID controller", *Proceeding of 2nd UKSIM European Symposium on Computer Modelling and Simulation*, pp. 40-45, 2008.

[5] W.Yim, "Adaptive Control of a Flexible Joint Manipulator", *IEEE International conference on Robotics and Automation*, pp. pp. 3441–3446., 2001.

[6] J. H. Oh, J.S. Lee, "Control of Flexible Joint Robot System by Backstepping Design Approach", *IEEE International Conference on Robotics and Automation*, Vol.4, pp. 3435-3440, 1997.

[7] F. Ghorbel, J. Y. Hung, M.W.Spong, "Adaptive Control of Flexible Joint Manipulators", *Control Systems Magazine*, Vol. 9, pp. 9-13, 1989.

[8] L.C. Lin, K.Yuan, "Control of Flexible Joint Robots via External Linearization Approach", *Journal of Robotic Systems*, Vol. 1 No.1, pp. 1-22, 2007.

[9] M. W. Spong, K. Khorasani, P. V. Kokotovic, "An Integral Manifold Approach to the Feedback Control of Flexible Joint Robots", *IEEE Journal of Robotics and Automation*, Vol. 3, No. 4, pp. 291-300, 1987.

[10] P. Tomei, "A Simple PD Controller for Robots with Elastic Joints", *IEEE Trans on Automatic Control*, Vol. 36, No. 10, pp. 1208-1213, 1991.

[11] J. S. Yeon, J. H. Park, "Practical Robust Control for Flexible Joint Robot Manipulators", *IEEE International Conference on Robotic and Automation*, pp. 3377-3382. 2008.

[12] M. A. Ahmad, R. M. T. Raja Ismail, M. S. Ramli and M. A. Zawawi, "Elastic Joint Control using Non-collocated Fuzzy and Filtering Scheme: A Comparative Assessment", *4th Asia International Conference on Mathematical/Analytical Modelling and Computer Simulation*, pp: 366-371, 2010.

[13] M. A. Ahmad, M.H. Suid, M. S. Ramli, M. A. Zawawi, R. M. T. Raja Ismail, "PD Fuzzy Logic with Non-collocated PID Approach for Vibration Control of Flexible Joint Manipulator", *6th International Colloquium on Signal Processing & Its Applications (CSPA)*, 2010.

[14] A. Jnifene,W. Andrews, "Experimental Study on Active Vibration Control of a Single-Link Flexible Manipulator Using Tools of Fuzzy Logic and Neural Networks", *IEEE Trans on Instrumentation and measurement*, Vol. 54, NO. 3, pp.1200-1208, 2005.

[15] M. A. Ahmad, R. M. T. Raja Ismail, M. S. Ramli, M. A. Zawawi, N. Hambali, and N. M. Abd. Ghani, "Vibration Control of Flexible Joint Manipulator using Input Shaping with PD-type Fuzzy Logic Control", *IEEE International*

Symposium on Industrial Electronics (ISlE 2009), pp.1184-1189, 2009.

[16] M.A. Ahmad, R.M.T. Raja Ismail, M.S. Ramli, "Optimal Control with Input Shaping for Input Tracking and Vibration Suppression of a Flexible Joint Manipulator", *European Journal of Scientific Research*, Vol. 28, No. 4, pp.583-599, 2009.

[17] M.A. Ahmad, M.S. Ramli, R.M.T. Raja Ismail, N. Hambali, M.A. Zawawi, "The investigations of input shaping with optimal state feedback for vibration control of a flexible joint manipulator", *Conference on Innovative Technologies in Intelligent Systems and Industrial Applications (CITISIA)*, pp.446-451, 2009.

[18] F. Farivar, M. Aliyari Shoorehdeli, M. A. Nekoui, M. Teshnehlab, "Sliding Mode Control of Flexible Joint Using Gaussian Radial Basis Function Neural Networks", *International Conference on Computer and Electrical Engineering'08*, *pp.856 – 860, 2008.*

[19] S. Ozgoli, H.D. Taghirad, "Design of Composite Control For Flexible Joint Robots With Saturating Actuators", *5th Iranian Conference on Fuzzy Systems*, pp.75-82, 2004.

[20] H. Chaoui, P. Sicard, A. Lakhsasi, "Reference model supervisoryloop for neural network based adaptive control of a flexible joint with hard nonlinearities", *IEEE Canadian Conference on Electrical and Computer Engineering*, vol. 4, pp. 2029–2034, 2004.

[21] D. Hui, S. Fuchun, S. Zengqi, "Observer-based adaptive controller design of flexible manipulators using time-delay neuro-fuzzy networks". *J. Intell. Robot. Syst.: Theory and Applications*, Vol. 34, No. 4, pp. 453–466, 2002.

[22] B. Subudhi, A.Morris, "Singular perturbation based neuro-h infinity control scheme for a manipulator with flexible links and joints. *Robotica* Vol. 24, No. 2, pp. 151–161, 2006.

[23] "Quanser Student Handout, Rotary Flexible Joint Module". *http://www.quanser.com*

[24] G.Chen and X.Dong, "From chaos to order: perspectives, methodologies and applications", *Singapore, World Scientific*, 1988.

[25] L. M. Pecora, T. L. Carroll, "Synchronization in chaotic systems", *Physics Review Letter*, Vol.64, pp.821–4, 1990.

[26] J. Yan, C. Li, "Generalized projective synchronization of a unified chaotic system", *Journal of Chaos, Solitons and Fractals*, Vol.26, pp.1119–24, 2005.

[27] J. P. Yan, C. P. Li, "Generalized projective synchronization for the chaotic Lorenz system and the chaotic Chen system", *J Shanghai Univ*, Vol.10, pp299, 2006.

[28] F. Farivar, M. Aliyari Shoorehdeli, M. A. Nekoui, M. Teshnehlab, "Generalized projective synchronization for chaotic systems via Gaussian Radial Basis Adaptive Backstepping Control", *Journal of Chaos, Solitons and Fractals* ,Vol. 42, pp.826–839, 2009.

[29] H. K. Chen, "Chaos and chaos synchronization of a symmetric gyro with linear-plus-cubic damping", *Journal of Sound and Vibration*, Vol. 255, pp.719–740, 2002.

[30] JE. Slotine, W. Li. "Applied nonlinear control", *New Jersey: Prentice-Hall, Englewood Cliffs*, 1991.

Biography of Authors

Maysam Zamani Pedram received B.Sc. degree in electrical engineering from K.N. Toosi University, Tehran, Iran in 2009. He is currently a M.Sc. student with Department of Electrical Engineering, K.N. Toosi University of Technology, Tehran, Iran. His research interests are Chaos, Robotics and Dynamics and Control of Non-Rigid body.

M. Aliyari Sh. received the B.Sc. degree in electronics engineering, the M.Eng. degree and Ph.D. degree in control engineering from K. N. Toosi University of Technology, in 2001, 2003 and 2008, respectively. He is currently an Assistant Professor with the Department of Mechatronics Engineering, K. N. Toosi University of Technology, Tehran. He is the author of more than 100 papers in international journals and conference proceedings. His research interests include Fault Tolerant, detection and diagnosis, Intelligent control of Mechatronics systems and Multi objective optimization.

Faezeh Farivar received the B.Sc. degree in Biomedical Engineering from Science and Research Branch, IAU, Tehran, Iran in 2004 and M.Sc. degree in Mechatronics Engineering from Science and Research Branch, IAU, Tehran, Iran in 2007. She is currently a Ph.D. Candidate of Control Engineering with Department of Mechatronics Engineering, Science and Research Branch, IAU, Tehran, Iran. Her research interests are in the areas of Mechatronics, chaotic systems, hybrid control, intelligent control, and application of control theory in biological systems.

Mojtaba Rostami. K received the B.Sc. degree in Control Engineering from Department of Electrical Engineering, K.N. Toosi University of Technology, Tehran, Iran in 2010. He is currently a M.Sc. student of Control Engineering with Department of Electrical and Computer Engineering, UT, Tehran, Iran. His research interests are in the areas of Mechatronics systems, hybrid control, and intelligent control.